The replica-symmetry-breaking solution of the Hopfield model at zero temperature: critical storage capacity and frozen field distribution

1994 J. Phys. A: Math. Gen. 27 4413

(http://iopscience.iop.org/0305-4470/27/13/016)

J. Phys. A: Math. Gen. 27 (1994) 4413–4424. Printed in the UK

The replica-symmetry-breaking solution of the Hopfield model at zero temperature: critical storage capacity and frozen field distribution

Kei Tokita†‡

Department of Pure and Applied Sciences, College of Arts and Sciences, University of Tokyo, Komaba 3-8-1, Meguro-ku, Tokyo 153, Japan

Received 25 January 1994

Abstract. The full replica-symmetry-breaking (RSB) solution of the Hopfield model at zero temperature ($T = 0$) is investigated. By using the RSB scheme by de Dominicis, Gabay and Orland, a free-energy functional in the so-called Sompolinsky gauge and variational equations are formulated. The resulting equations are conveniently defined for numerical analysis since a singularity at $T = 0$ is formally avoided. Elaborate numerical analyses provide a corrected storage capacity, order parameter functions and the frozen field distribution both in the spin-glass phase and the ferromagnetic retrieval phase.

1. Introduction

Since the Hopfield model [1, 2] and its family of neural network models [3, 4] have been fully researched in the context of the spin-glass (SG) theory [5, 6] and other new techniques of analysis [7], studies on the Hopfield model itself may seem to have a rather classical flavour nowadays. However, there are still important open problems: low-temperature behaviour in the phase where the replica-symmetric (RS) solutions are unstable and, in particular, the critical storage capacity (α_c) in the low-temperature limit ($T = 1/\beta \to 0$). This paper discusses the RSB solution of the Hopfield model in order to consider such topics.

The free energy of the Hopfield model has been introduced by Amit *et al* (AGS) [2] as

$$f_n = \frac{\alpha}{2} + \frac{1}{2n}\sum_{\nu=1}^{s}\sum_{a=1}^{n}(m_a^\nu)^2 + \frac{\alpha}{2\beta n}\mathrm{Tr}\ln[(1-\beta)\mathbf{I} - \beta\mathbf{Q}] + \frac{\alpha\beta}{2n}\sum_{a\neq b}^{n} r_{ab}q_{ab} - \frac{1}{n\beta}\langle\!\langle \ln Z_0 \rangle\!\rangle \qquad \text{as} \quad n \to 0 \tag{1}$$

where

$$Z_0 = \mathrm{Tr}_{\{n\}}\exp\beta\left(\frac{\alpha\beta}{2}\sum_{a\neq b}^{n} r_{ab}S^aS^b + \sum_{a=1}^{n} h_aS^a\right) \tag{2}$$

$$h_a = \sum_{\nu=1}^{s}(m_a^\nu + h^\nu)\xi^\nu . \tag{3}$$

† E-mail address: tokita@complex.c.u-tokyo.ac.jp

‡ Present address: Department of Physics, Faculty of Science, Osaka University, Toyonaka, Osaka 560, Japan.

0305-4470/94/134413+12$19.50

Here $\alpha(\equiv p/N)$ denotes the rate of memory loading, p the number of random patterns for memories and N the system size. $\mathbf{I}$ is a unit matrix with $n \times n$ elements while $\mathbf{Q} = \{q_{ab}\}$ is a replica matrix which gives the SG order parameter. m_a^ν denotes the macroscopic order parameter which roughly becomes unity in the so-called 'ferromagnetic retrieval (FMR)' phase, where the system maintains a capacity of an associative memory, while $m_a^\nu = 0$ in the SG phase, having no overlap with any memorized pattern. By $\mathrm{Tr}_{\{n\}}$ we denote explicitly that the trace is taken over n-replicated binomial spins. Here we note that the average

$$\langle\langle O\{\xi^\nu\}\rangle\rangle \equiv \frac{1}{2^s}\sum_{\nu=1}^{s}\sum_{\xi^\nu=\pm 1} O\{\xi^\nu\} \tag{4}$$

denotes the random average for ($s \ll p$) 'condensed patterns'.

AGS have shown that the RS solution is stable in almost all regions which belong to the FMR phase, and by extrapolating to the RSB region they derived the mean-field equations at $T = 0$ and determined $\alpha_c = 0.138$. Crisanti *et al* [8], moreover, have examined the one-step RSB solution and have corrected α_c from 0.138 to 0.144. However, at $T = 0$ both the RS solution and the RSB solution become unstable when only a finite number of steps is used. Therefore the full (infinite step) RSB solution should be considered. Moreover, only the full RSB discussion provides us with an appropriate estimation for the order parameter functions and the frozen field distribution which is expected to give some helpful information if one addresses oneself to dynamical profiles [9, 10].

In section 2, the RSB scheme by de Dominicis *et al* (DGO) [11–13] is examined with the help of the so-called Sompolinsky gauge [14]. DGOs RSB scheme uses a different replica matrix (*the DGO matrix*) from the one employed in Parisi's RSB scheme [15, 16]. In particular, in subsection 2.1, the diagonalization of the DGO matrix is outlined because the corresponding terms in the free energy only appear in the Hopfield model, and not in the SK model [17] which was investigated in the RSB discussions of [11, 12, 15]. Here we note that the resulting 'gauge invariance' of the free energy functional plays an important role since it enables us to solve numerically the variational equations avoiding a singularity originating at $T = 0$. Such a numerical solution at $T = 0$ cannot be achieved within the framework of Parisi's RSB scheme. In section 3, we solve numerically the variational equations at $T = 0$ for both the SG and FMR phases for several values of α near α_c. The results are summarized and discussed in section 4.

2. The full RSB formulation

2.1. *Diagonalization of the* DGO *matrix*

Here let us concentrate on calculating the third and fourth terms in the free energy (1) with the help of DGOs RSB scheme. The essence of the following calculation is the diagonalization of the DGO matrix. In the scheme, the $n \times n$ dimensional DGO matrix $\mathbf{Q}$ in (1) is recursively defined as

$$\mathbf{Q} = \begin{pmatrix} \mathbf{Q}_0 - \mathbf{D}_0 & \mathbf{Q}_0 & \cdots & \mathbf{Q}_0 \\ \mathbf{Q}_0 & \mathbf{Q}_0 - \mathbf{D}_0 & \cdots & \mathbf{Q}_0 \\ \vdots & \vdots & \ddots & \vdots \\ \mathbf{Q}_0 & \cdots & \cdots & \mathbf{Q}_0 - \mathbf{D}_0 \end{pmatrix} \tag{5}$$

where $\mathbf{Q}_0$ and $\mathbf{D}_0$ are the $p_0 \times p_0$ Parisi matrices. In general, a Parisi matrix $\mathbf{A}_0$ of level K (which should be infinity later) is recursively defined as the Kth iterate of

$$\mathbf{A}_k = \begin{pmatrix} \mathbf{A}_{k+1} & a_k\mathbf{U}_{k+1} & \cdots & a_k\mathbf{U}_{k+1} \\ a_k\mathbf{U}_{k+1} & \mathbf{A}_{k+1} & \cdots & a_k\mathbf{U}_{k+1} \\ \vdots & \vdots & \ddots & \vdots \\ a_k\mathbf{U}_{k+1} & a_k\mathbf{U}_{k+1} & \cdots & \mathbf{A}_{k+1} \end{pmatrix} \tag{6}$$

with $\mathbf{A}_{K+1} = \tilde{a}$ representing the value of the diagonal elements. $\mathbf{U}_k$ denotes the $p_k \times p_k$ matrix whose elements are all 1. Each matrix $\mathbf{A}_k$ is specified by its dimension p_k and the coefficient a_k of non-diagonal submatrices $\mathbf{U}_{k+1}$. Thus a Parisi matrix $\mathbf{A}_0$ is determined by the series of integers $p_0 > p_1 > \cdots > p_K > p_{K+1} = 1$, where naturally p_k needs to divide p_{k-1} in order for successive submatrices to fit correctly, and the series of coefficients $\{a_0, a_1, \ldots, a_K, a_{K+1} = \tilde{a}\}$. Here we note that p_0 needs to divide n and that the diagonal elements of $\mathbf{Q}_0$ and $\mathbf{D}_0$ are $\tilde{q} = q_K$ and $\tilde{d} = d_K + q_K$. To get a proper solution, one should take the limits $p_0 \gg p_1 \gg \cdots \gg p_K \to \infty$ (we will call this *the DGO limit*) and $K \to \infty$ before $n \to 0$.

First, let us consider the term $\Phi \equiv 1/n \sum_{a \neq b}^{n} r_{ab}q_{ab}$ in (1). We will denote the diagonal and off-diagonal submatrix of the DGO matrix $\mathbf{R} = \{r_{ab}\}$ by $\mathbf{R}_0$ and $\mathbf{E}_0$ which are parameterized by $\{r_i\}$ and $\{e_i\}$, respectively, in the same way as $\mathbf{Q}_0$ and $\mathbf{D}_0$ in $\mathbf{Q}$. Consequently, Φ can be represented as

$$\begin{aligned}
\Phi &= \frac{1}{n}\mathrm{Tr}\,\mathbf{RQ} = \frac{1}{p_0}\left[\mathrm{Tr}\,(\mathbf{R}_0 - \mathbf{E}_0)(\mathbf{Q}_0 - \mathbf{D}_0) + (n/p_0 - 1)\mathrm{Tr}\,\mathbf{R}_0\mathbf{Q}_0\right] \\
&= \frac{1}{p_0}\left[\frac{n}{p_0}\mathrm{Tr}\,\mathbf{Q}_0\mathbf{R}_0 - \mathrm{Tr}\,\mathbf{D}_0\mathbf{R}_0 - \mathrm{Tr}\,\mathbf{Q}_0\mathbf{E}_0 + \mathrm{Tr}\,\mathbf{D}_0\mathbf{E}_0\right] \\
&= \frac{n}{p_0}\left(\sum_{l=0}^{K}(q_l r_l - q_{l-1}r_{l-1})p_l - q_K r_K + \tilde{q}\,\tilde{r}\right) \\
&\quad - \left(\sum_{l=0}^{K}(d_l r_l - d_{l-1}r_{l-1})p_l - d_K r_K + \tilde{d}\,\tilde{r}\right) \\
&\quad - \left(\sum_{l=0}^{K}(q_l e_l - q_{l-1}e_{l-1})p_l - q_K e_K + \tilde{q}\,\tilde{e}\right) \\
&\quad + \sum_{l=0}^{K}(d_l e_l - d_{l-1}e_{l-1})p_l - d_K e_K + \tilde{d}\,\tilde{e} \\
&= -q_K r_K - \sum_{l=0}^{K}(\Delta_l^{(r)} q_l + \Delta_l^{(q)} r_l) \\
&\to -q(1)r(1) - \frac{1}{\beta}\int_0^1 (\dot{\Delta}_r(x)q(x) + \dot{\Delta}_q(x)r(x))\mathrm{d}x
\end{aligned} \tag{7}$$

where dots denote derivatives with respect to x. In the above calculation, by Tr we explicitly denote that the summation is taken over all the elements of the Parisi matrix as

$$\frac{1}{p_0}\mathrm{Tr}\,\mathbf{A}_0 = \frac{1}{p_0}\sum_{a,b}^{p_0} A_{0,ab} = \sum_{i=0}^{K}(a_i - a_{i-1})p_i - a_K + \tilde{a} \qquad a_{-1} \equiv 0 \tag{8}$$

where $A_{0,ab}$ denotes the (a, b) element of the $p_0 \times p_0$ Parisi matrix. Furthermore, we used $d_l - d_{l-1} = \Delta_l^{(q)}/p_l$, $e_l - e_{l-1} = \Delta_l^{(r)}/p_l$, $\Delta_l^{(q)} \to \dot{\Delta}_q(x)\mathrm{d}x/\beta$ and $\Delta_l^{(r)} \to \dot{\Delta}_r(x)\mathrm{d}x/\beta$

[12, 13] in the DGO limit, $K \to \infty$ and $l/K \to x$. $\Delta_r(x)$ and $\Delta_q(x)$ correspond to Sompolinsky's non-ergodicity functions [14] determining the gauge of x [12, 18] together with $r(x)$ and $q(x)$, respectively, as $x = -T\dot{\Delta}_q(x)/\dot{q}(x) = -T\dot{\Delta}_r(x)/\dot{r}(x)$ (Parisi's x). Here we note that these functions are scaled by β since the Parisi equations (21) and (23) to appear later are scaled in the same way.

Second, let us consider the diagonalization of the DGO matrix as a preliminary for calculating the term $L \equiv 1/n\mathrm{Tr}\ \ln[(1-\beta)\mathbf{I}) - \beta\mathbf{Q}]$ in (1). Since the Parisi matrices $\mathbf{Q}_0$ and $\mathbf{D}_0$ commutate [16], one can write the common eigenvector $\mathbf{u}_\lambda$ of $\mathbf{Q}_0$ and $\mathbf{D}_0$ as

$$\begin{pmatrix} \mathbf{Q}_0 - \mathbf{D}_0 & \mathbf{Q}_0 & \cdots & \mathbf{Q}_0 \\ \mathbf{Q}_0 & \mathbf{Q}_0 - \mathbf{D}_0 & \cdots & \mathbf{Q}_0 \\ \vdots & \vdots & \ddots & \vdots \\ \mathbf{Q}_0 & \cdots & \cdots & \mathbf{Q}_0 - \mathbf{D}_0 \end{pmatrix} \begin{pmatrix} c_1\mathbf{u}_\lambda \\ c_2\mathbf{u}_\lambda \\ \vdots \\ c_m\mathbf{u}_\lambda \end{pmatrix} = \epsilon_\lambda \begin{pmatrix} c_1\mathbf{u}_\lambda \\ c_2\mathbf{u}_\lambda \\ \vdots \\ c_m\mathbf{u}_\lambda \end{pmatrix} \tag{9}$$

where $m = n/p_0$ and ϵ_λ denote the eigenvalues of $\mathbf{Q}$. Consequently, with respect to the coefficients $c_1, c_2, \cdots, c_m$, one can obtain that

$$\begin{pmatrix} \lambda_q - \lambda_d & \lambda_q & \cdots & \lambda_q \\ \lambda_q & \lambda_q - \lambda_d & \cdots & \lambda_q \\ \vdots & \vdots & \ddots & \vdots \\ \lambda_q & \cdots & \cdots & \lambda_q - \lambda_d \end{pmatrix} \begin{pmatrix} c_1 \\ c_2 \\ \vdots \\ c_m \end{pmatrix} = \epsilon_\lambda \begin{pmatrix} c_1 \\ c_2 \\ \vdots \\ c_m \end{pmatrix} \tag{10}$$

where λ_q and λ_d denote the eigenvalues of $\mathbf{Q}_0$ and $\mathbf{D}_0$, respectively. Thus, the eigenvalue ϵ_λ of the DGO matrix is represented by

$$\epsilon_0 = m\lambda_q - \lambda_d \qquad \text{non-degenerate} \tag{11}$$

$$\epsilon_l = -\lambda_d \qquad l = 1, 2, \cdots, m-1 \qquad (m-1)\text{-fold degenerate}. \tag{12}$$

The eigenvalues of a Parisi matrix are known [19, 20] to be

$$\lambda_{p_0} = \sum_{i=0}^{K}(p_i - p_{i+1})a_i + \tilde{a} \tag{13}$$

which is non-degenerate, and

$$\lambda_k = \sum_{i=k}^{K}(p_i - p_{i+1})a_i - p_k a_k + \tilde{a} \tag{14}$$

which is $p_0(1/p_{k+1} - 1/p_k)$-fold degenerate for each $k(k = 0, 1, \cdots, K)$. By substituting (13) and (14) into (11) and (12), the eigenvalues of the DGO matrix therefore can be obtained as

$$\epsilon_{0,p_0} = -\sum_{i=0}^{K}\Delta_i^{(q)} - q_K + \frac{n}{p_0}\left\{\sum_{j=0}^{K}(p_j - p_{j+1})q_j + q_K\right\} \tag{15}$$

$$\epsilon_{0,k} = -\sum_{i=k+1}^{K}\Delta_i^{(q)} - q_K + \frac{n}{p_0}\left\{\sum_{j=k}^{K}(p_j - p_{j+1})q_j + q_K - p_k q_k\right\} \tag{16}$$

$$\epsilon_{l,p_0} = -\sum_{i=0}^{K}\Delta_i^{(q)} - q_K \tag{17}$$

$$\epsilon_{l,k} = -\sum_{i=k+1}^{K}\Delta_i^{(q)} - q_K \tag{18}$$

where $k = 0, 1, \ldots, K$. We also used $\Delta_i^{(q)} \equiv p_i(d_i - d_{i-1})$ [13]. The numbers of degeneracy of ϵ_{0,p_0}, $\epsilon_{0,k}$, ϵ_{l,p_0} and $\epsilon_{l,k}$ are 1, $p_0(1/p_{k+1} - 1/p_k)$, $n/p_0 - 1$ and $(n - p_0)(1/p_{k+1} - 1/p_k)$, respectively. The total number of degeneracy is n as can be easily checked. Now it is possible to obtain the term $L \equiv 1/n\mathrm{Tr}\ln[(1-\beta)\mathbf{I}) - \beta\mathbf{Q}]$ in the continuum limit by substituting the above eigenvalues in L and taking the proper limits. The details of the limitation process are similar to the ones in [19] or the same ones can be referred to [21].

2.2. *Free-energy functional and the generalized Parisi equations*

By the calculations in the previous subsection and others for the Parisi equation [15], the free energy for the Hopfield model in the *Sompolinsky gauge* can be represented as a functional:

$$\begin{aligned} f_s = {} & \tfrac{1}{2}\alpha + \tfrac{1}{2}\sum_{\nu}^{s}(m^\nu)^2 + \tfrac{1}{2}\alpha\beta\, r(1)\,(1-q(1)) \\ & - \tfrac{1}{2}\alpha\int_0^1 \left(\dot{\Delta}_r(x)q(x) + \dot{\Delta}_q(x)r(x)\right)\mathrm{d}x \\ & - \int_{-\infty}^{\infty}\frac{\mathrm{d}z}{\sqrt{2\pi r(0)}}\left\langle\!\!\left\langle \exp\left(\frac{-(z-h)^2}{2r(0)}\right)\right\rangle\!\!\right\rangle \varphi(0,z) \\ & + \frac{\alpha}{2\beta}\left\{\frac{-\beta q(0)}{1-\chi(0)} + \ln[1-\chi(1)] - \int_0^1 \mathrm{d}x\,\frac{\beta\dot{q}(x)}{1-\chi(x)}\right\} \\ & + \int_{-\infty}^{\infty}\mathrm{d}z P(1,z)\left\{\varphi(1,z) - \frac{1}{\beta}\ln 2\cosh\sqrt{\alpha}\beta z\right\} \\ & - \int_0^1 \mathrm{d}x\int_{-\infty}^{\infty}\mathrm{d}z P(x,z)\left\{\dot{\varphi} + \tfrac{1}{2}\dot{r}(x)\varphi'' - \tfrac{1}{2}\dot{\Delta}_r(x)2\varphi'^2\right\} \end{aligned} \tag{19}$$

which is maximized by the order parameter functions $r(x)$, $q(x)$, $\Delta_r(x)$, $\Delta_q(x)$, $\varphi(x,z)$, $P(x,z)$ and minimized by m^ν. Dots and primes denote the derivatives with respect to x and z, respectively. Here $q(x)$ and $r(x)$ correspond to the order parameters in the continuum limit, i.e. the SG order parameter function and the order parameter function describing the noise due to the *uncondensed* patterns, respectively. m^ν denotes the average overlap of the states and the νth memorized pattern. The term involving $\chi(x) \equiv \beta(1-q(1)) + \Delta_q(x) - \Delta_q(1)$ corresponds to $L \equiv 1/n\mathrm{Tr}\ln[(1-\beta)\mathbf{I}) - \beta\mathbf{Q}]$ in the continuum limit mentioned in the previous subsection. The last two terms, including the function $\varphi(x,z)$, are introduced via a Lagrange multiplier function $P(x,z)$ in the scheme for numerical analysis by Sommers *et al* [18], Nemoto [22] and the author [19]. Those two terms should vanish when the maximum of the free energy is reached. The derivations are similar to the case for SG models [12, 13, 15, 23]. The definition of the local field h is given as

$$h = \frac{1}{\sqrt{\alpha}}\sum_{\nu=1}^{s}(m^\nu + h^\nu)\xi^\nu . \tag{20}$$

With regard to Sompolinsky's non-ergodicity functions [14] $\Delta_r(x)$ and $\Delta_q(x)$, we note that the free energy (19) is 'gauge invariant' since (19) and its variational equations still hold if x is replaced by some *monotonic* function $u(x)$ with $u(0) = 0$ and $u(1) = 1$.

Now, the generalized 'Parisi equations' for the Hopfield model can be obtained by taking the functional derivatives of (19) with respect to the order parameter functions after

the variable transformations $\sqrt{\alpha}\dot{\Delta}_r(x) \to \dot{\Delta}_r(x)$ and $\sqrt{\alpha}\dot{\Delta}_q(x) \to \dot{\Delta}_q(x)$ as

$$\dot{M} = -\tfrac{1}{2}\dot{r}(x)M'' + \dot{\Delta}_r(x)MM' \qquad M \equiv \frac{\varphi'}{\sqrt{\alpha}} \tag{21}$$

$$M(1,z) = \tanh\tilde{\beta}z \tag{22}$$

$$\dot{P} = \tfrac{1}{2}\dot{r}(x)P'' + \dot{\Delta}_r(x)(PM)' \tag{23}$$

$$P(0,z) = \left\langle\!\!\left\langle \frac{1}{\sqrt{2\pi r(0)}} \exp\left(-\frac{(z-h)^2}{2r(0)}\right)\right\rangle\!\!\right\rangle \tag{24}$$

$$q(x) = \int_{-\infty}^{\infty} \mathrm{d}z\, P(x,z)M(x,z)^2 \tag{25}$$

$$\tilde{\beta}(1-q(1)) + \Delta_q(x) - \Delta_q(1) = \int_{-\infty}^{\infty} \mathrm{d}z\, P(x,z)M'(x,z) \tag{26}$$

$$\chi(x) = \frac{1}{\sqrt{\alpha}}\left[\tilde{\beta}(1-q(1)) + \Delta_q(x) - \Delta_q(1)\right] \tag{27}$$

$$\dot{r}(x) = \frac{\dot{q}(x)}{[1-\chi(x)]^2} \tag{28}$$

$$\dot{\Delta}_r(x) = \frac{\dot{\Delta}_q(x)}{[1-\chi(x)]^2} \tag{29}$$

$$m^{\nu} = \int_{-\infty}^{\infty} \mathrm{d}z M(0,z)\left\langle\!\!\left\langle \xi^{\nu} \frac{1}{\sqrt{2\pi r(0)}} \exp\left(-\frac{(z-h)^2}{2r(0)}\right)\right\rangle\!\!\right\rangle \tag{30}$$

$$\tilde{\beta} \equiv \sqrt{\alpha}\beta\,. \tag{31}$$

In the above formalism $P(1,z)$ gives the internal field distribution. When we consider only one condensed pattern($s=1$) and $h^1 = 0$, we can estimate the sample average $\langle\!\langle \cdots \rangle\!\rangle$ in (24) and (30), and obtain the following equations:

$$P(0,z) = \frac{1}{\sqrt{2\pi r(0)}} \exp\left(-\frac{(z-m/\sqrt{\alpha})^2}{2r(0)}\right) \tag{32}$$

$$m = \int_{-\infty}^{\infty} \mathrm{d}z M(1,z)P(1,z) \tag{33}$$

where we have written m^1 as m and have used $m = \int_{-\infty}^{\infty} \mathrm{d}z M(x,z)P(x,z) = \text{constant}$. It is noted that (32) and (33) coincide with the corresponding equations for the SK model [17, 22] in a magnetic field. Consequently, in the same way as for the SK model, the field distribution is found to be a non-trivial function $P(x,z)$ which is clearly different from the Gaussian distribution obtained by the RS solution.

Here we note that differentiation of the two functions $q(x)$ (equation (25)) and $\Delta_q(x)$ (equation (26)) with respect to x gives for $\dot{\Delta}_q(x), \dot{q}(x) \neq 0$ the equation for the condition for marginal stability in replica space [2, 19]:

$$1 = \frac{1}{[1-\chi(x)]^2} \int_{-\infty}^{\infty} \mathrm{d}z P(x,z)M'(x,z)^2\,. \tag{34}$$

By differentiating once more, one can obtain an equation

$$0 = \dot{q}(x)\int_{-\infty}^{\infty} \mathrm{d}z P(x,z)M''(x,z)^2 + 2\,\dot{\Delta}_q(x)\left[\int_{-\infty}^{\infty} \mathrm{d}z P(x,z)M'(x,z)^2 + [1-\chi(x)]^3/\sqrt{\alpha}\right] \tag{35}$$

which denotes that (25) and (26) are essentially equivalent; those two equations determine only the gauge relation between $q(x)$ and $\Delta_q(x)$ (e.g. the Parisi gauge is given by $\dot{\Delta}_q(x) = -\tilde{\beta}x\dot{q}(x)$, providing us with the variational equations for the Hopfield model with Parisi's RSB scheme [19]). This gauge relation also holds for the pair of $r(x)$ and $\dot{\Delta}_r(x)$ via (28) and (29).

In the limit $\beta \to \infty$, one can easily see that (22), (25) and (26) reduce to

$$M(1,z) = 2\theta(z) - 1 \tag{36}$$

$$M'(1,z) = 2\delta(z) \tag{37}$$

$$q(1) = \int_{-\infty}^{\infty} \mathrm{d}z\, P(1,z) = 1\,. \tag{38}$$

Moreover, by substituting (38) into (26) and (27) and setting $x = 1$, one has

$$\sqrt{\alpha}\chi(1) = \tilde{\beta}\left[1 - q(1)\right] = P(1,0) = 0 \tag{39}$$

which is also supported by numerical studies of the SK model in an external field [24]. Thus it is found that the two functions $\chi(x)$ and $\Delta_q(x)$ are essentially equivalent

$$\Delta_q(x) = \sqrt{\alpha}\chi(x) = \int_{-\infty}^{\infty} \mathrm{d}z P(x,z) M'(x,z) \tag{40}$$

where we set $\Delta_q(1) = 0$ according to definition [14].

3. Numerical analysis at $T = 0$

For several values of α, we have solved (21)–(33) with (36)–(40) at $T = 0$ numerically both for the SG phase and the FMR phase. Since we can interpret the linear terms of (21) and (23) as diffusion equations, by introducing the Green function, the nonlinear partial differential equations (21), (23), (32) and (36) can be transformed to the following integral equations at $T = 0$:

$$G(x,z;\tilde{x},\tilde{z}) = \frac{1}{\sqrt{2\pi(r(\tilde{x}) - r(x))}} \exp\left(-\frac{(z-\tilde{z})^2}{2(r(\tilde{x}) - r(x))}\right) \tag{41}$$

$$M(x,z) = \mathrm{erf}\left(\frac{z}{\sqrt{2(r(1) - r(x))}}\right) - \int_x^1 \mathrm{d}\tilde{x}\,\dot{\Delta}_r(\tilde{x}) \int_{-\infty}^{\infty} \mathrm{d}\tilde{z} G(x,z;\tilde{x},\tilde{z}) M(\tilde{x},\tilde{z}) M'(\tilde{x},\tilde{z}) \tag{42}$$

$$P(x,z) = \frac{1}{\sqrt{2\pi r(x)}} \exp\left(-\frac{(y - m/\sqrt{\alpha})^2}{2r(x)}\right) + \int_0^x \mathrm{d}\tilde{x}\,\dot{\Delta}_r(\tilde{x}) \times \int_{-\infty}^{\infty} \mathrm{d}\tilde{z} G(\tilde{x},\tilde{z};x,z)\,(M(\tilde{x},\tilde{z})P(\tilde{x},\tilde{z}))' \tag{43}$$

where $\mathrm{erf}(x) \equiv 2/\pi \int_0^x \exp(-t^2)\mathrm{d}t$ denotes the error function. This enables us to obtain M, P, m, r, q and χ by means of an iterative procedure in the order (42) $\to$ ((32) $\rightleftharpoons$ (33)) $\to$ (43) $\to$ (25) $\to$ (28) $\to$ (42) $\cdots$. In the SG phase, $\Delta_q(x)$ ($\Delta_r(x)$, $\chi(x)$) can be determined *a priori* by choosing a special gauge of x. On the other hand, in the FMR phase, $\Delta_q(x)$ has to be determined through (40) at each step of the iterative procedure. Details are explained in the following subsections for each phase.

For numerical integration and differentiation we have discretized the variable x, dividing the interval $[0, 1]$ into $40 \sim 100$ pieces. The variable z is also discretized, dividing the interval $[-A, A]$ into 100 pieces, where the value of A is determined differently for $P(x,z)$ and $M(x,z)$ because $P(x,z)$ spreads over a wider range of z than $M(x,z)$ which is expected

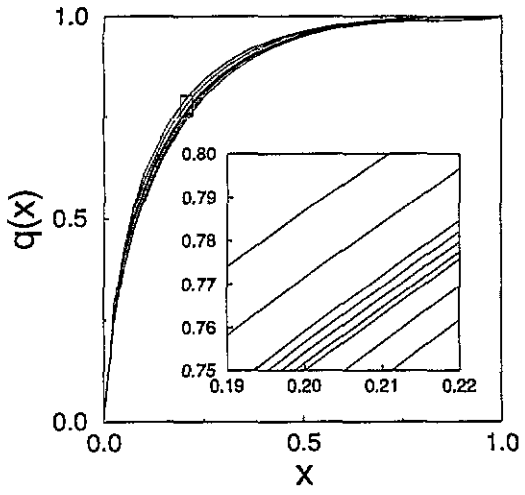

Figure 1. Order parameter function $q(x)$ at $T = 0$ in the SG phase for $\alpha = 0.1, 0.12, 0.14, 0.145, 0.15, 0.155, 0.16, 0.18$ and 0.2 (top to bottom).

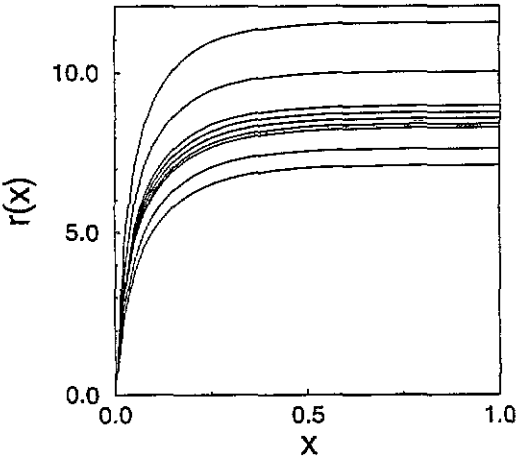

Figure 2. Order parameter function $r(x)$ at $T = 0$ in the SG phase for $\alpha = 0.1, 0.12, 0.14, 0.145, 0.15, 0.155, 0.16, 0.18$ and 0.2 (top to bottom).

to change its value drastically near $z = 0$ (i.e. very close to a step function, especially in the FMR phase), e.g. $A = 12.0$ and $A = 0.05$ for $P(x, z)$ and $M(x, z)$, respectively. Furthermore, we have used a cubic spline for interpolation. Quadratic functions and hyperbolic tangents are also used for extrapolations of $\ln(P(x, z))$ and $M(x, z)$, respectively, both defined on the entire range of z. We have carried out the above iterative procedure until the maximum variance of all the variables P, M, r, q and χ is less than 10^{-6}.

Once a set of solutions (m, q, r, χ, P, M) for a value of α is obtained, a new solution at an adiabatically shifted value of α is calculated (i.e. the previously obtained solutions are included as an initial condition). Thus one can detect the vanishing point of the metastable states corresponding to the FMR phase and obtain α_c.

3.1. SG solution

Let us take a closer look at the solutions in the SG phase. Here we note that $\Delta_q(0)$ in the SG phase depends only on α as $\Delta_q(0) = \sqrt{\alpha}/(1 + \sqrt{\alpha})$ [2], which is independent of the temperature. Therefore one can see that $\Delta_q(0) \to 1$ in the 'SK limit ($\sqrt{\alpha} \to \infty$)' [19].

Consequently the special gauge

$$\Delta_q(x) = \sqrt{\alpha}(1-x)/(1+\sqrt{\alpha}) \tag{44}$$

is used for numerical analyses.

For several values of α in the SG phase, $q(x)$ and $r(x)$ are shown in figures 1 and 2, respectively, where $q(0) = r(0) = 0$ denotes $m = 0$. The frozen field distribution $P(1, z)$ is depicted in figure 3 in which we see the symmetry and the typical form of a double-peak. It is clarified for the SG phase that the order parameter functions and frozen field distribution do not vary drastically around α_c. Hence the disappearance of the metastable FMR states does not affect the SG phase.

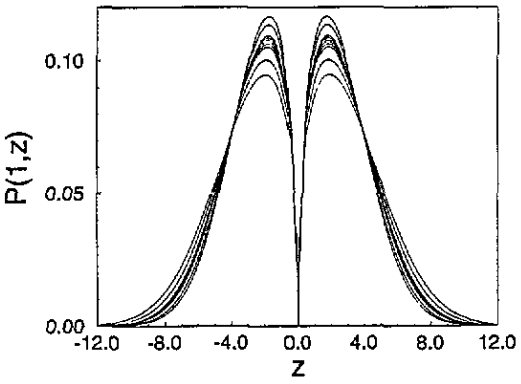

Figure 3. The frozen field distribution $P(1, z)$ at $T = 0$ in the SG phase for $\alpha = 0.1$, 0.12, 0.14, 0.145, 0.15, 0.155, 0.16, 0.18 and 0.2 (bottom to top).

Here we note that $P(1, z)$ in the SG phase has a non-trivial form and cannot be approximated by any Gaussian distribution at all. This is the main reason why one cannot describe the dynamics of the Hopfield model by a finite number of macroscopic time-dependent order parameters in such a way that it converges to the spurious state or the SG state, while one can approximately describe a dynamics which converges to the FMR states [9, 25].

3.2. *FMR solution*

In the FMR phase, since a dependency of $\chi(0)$ on α is not given explicitly as in the SG phase mentioned above, $\chi(0)$ has to be determined self-consistently during the numerical calculations. Therefore we apply the special gauge

$$\chi(x) = \chi(0)(1-x) \tag{45}$$

where $\chi(0)$ is reset by (40) during each step of the iterative procedure. The values for $\chi(0)$ are shown in figure 4 together with the ones obtained by the RS discussion.

For several values of α in the FMR phase, $q(x)$ and $r(x)$ are shown in figures 5 and 6, respectively. We note that in figure 5(a), the $q(x)$ for $\alpha = 0.1, 0.11, 0.12$ are so close to unity that it is difficult to distinguish them. Therefore, at $\alpha < 0.13$ the RS solutions are almost recovered, although $q(0) \neq 1$ even at $\alpha = 0.1$. On the other hand, $q(x)$ in the FMR phase shows a typical dependency on α near α_c. In particular, $q(0)$ decreases as $\alpha \to \alpha_c$, showing that the variety of overlaps between two pure states increases abruptly near α_c (figure 5(b)). Consequently the transition where the FMR states (dis)appear is accompanied with an abrupt (dis)appearance of many pure states which have different patterns of spin configurations but the same macroscopic overlaps with one of the memorized patterns. The $r(x)$ for several values of α in figure 6(a) look like a straight line, i.e. the RS solution,

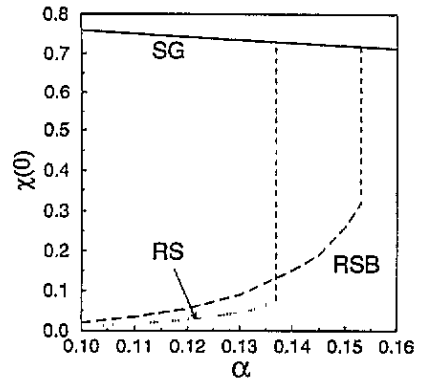

Figure 4. $\chi(0)$ versus α.

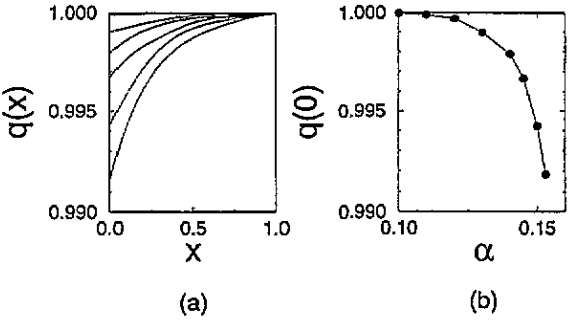

Figure 5. Order parameter function at $T = 0$ in the FMR phase: (*a*) $q(x)$ for $\alpha = 0.1$, 0.11, 0.12, 0.13, 0.14, 0.145, 0.15 and 0.153 (top to bottom), (*b*) $q(0)$ versus α.

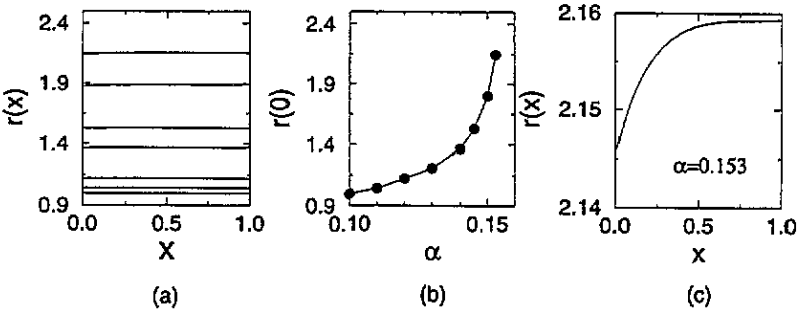

Figure 6. Order parameter function at $T = 0$ in the FMR phase: (*a*) $r(x)$ for $\alpha = 0.1$, 0.11, 0.12, 0.13, 0.14, 0.145, 0.15 and 0.153 (bottom to top), (*b*) $r(0)$ versus α, (*c*) $r(x)$ for $\alpha = 0.153$.

however, they exactly show RSB respectively. For example, $r(x)$ for $\alpha = 0.153$ is depicted in figure 6(*c*).

The frozen field distribution $P(1, z)$ for several values of α are given in figure 7 in which we can see the broken symmetry. Their main peak is nearly Gaussian but they have a second peak as was also the case in figure 3.

The percentage of errors, $(1-m)/2$, in the FMR phase is shown in figure 8 as a function of α at $T = 0$. For comparison, the results of the present calculations are plotted together with the predictions of the RS theory [2] and the one-step RSB theory [8]. It can clearly be seen that α_c is somewhat higher than the values obtained by the RS (0.138) and one-step RSB

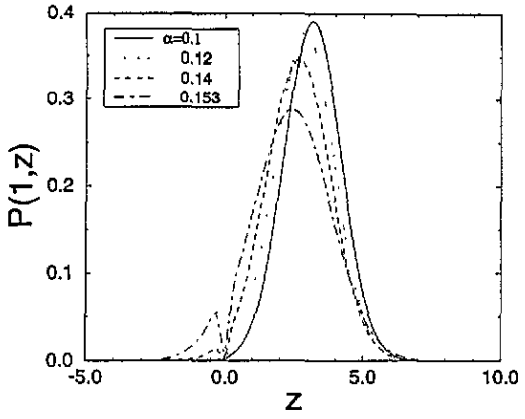

Figure 7. Frozen field distribution $P(1,z)$ at $T = 0$ in the FMR phase for $\alpha = 0.1$, 0.12, 0.14 and 0.153.

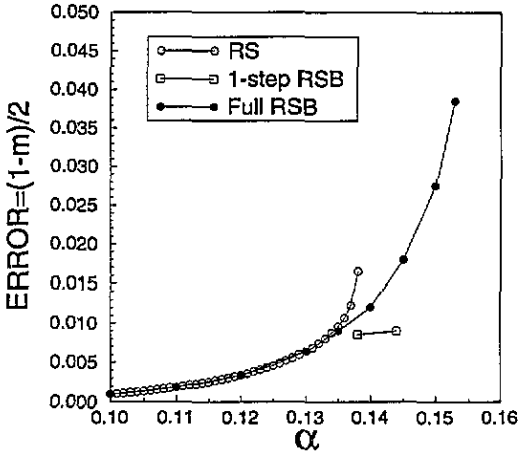

Figure 8. Percentage of errors $(1 - m)/2$.

(0.144) theories. We determined α_c in the following way. At $\alpha = 0.153$ the RSB solution with finite m was found, on the other hand, at $\alpha = 0.157$ and beyond, no RSB solution with finite m was found. At $0.153 < \alpha < 0.157$, the calculation converges to an unexpected solution, therefore, it is concluded that $\alpha_c = 0.155 \pm 0.002$.

These results are remarkable in the sense that the full RSB is observed even in the FMR phase, and the order parameter functions and the frozen field distribution are explicitly determined for αs.

4. Summary and discussion

We have formulated the RSB solution of the Hopfield model with the Sompolinsky gauge at $T = 0$ and obtained the variational equations. Extensive numerical analyses were carried out, both for the SG and the FMR phases, in the most interesting region where the FMR phase disappears. The first result of this paper is that the storage capacity α_c at $T = 0$ is corrected to a value which is higher than the ones obtained by the RS and one-step RSB discussions. Our result is the first self-consistent estimation of the critical storage capacity using the full RSB scheme. Another interesting aspect of this result is that it also indicates that RSB promotes the stability of the FMR solution against the increase of the so-called 'slow' or 'stochastic synaptic' noise [3] originating in αs increase. The second major result of this

paper is that the frozen field distribution (FFD) $P(1, z)$ is corrected to a non-Gaussian form for both the SG phase and the FMR phase. It is found that the FFD for the FMR phase is only slightly different from the Gaussian form obtained in the RS discussion. Therefore, as far as the FMR phase is concerned, the AGS theory is able to go beyond the RS approximation even at $T = 0$. This situation also explains why the dynamical evolution of m in the FMR phase can approximately be described by only a few macroscopic variables [9, 10]. However, we note that the FFD for the SG phase cannot be fitted by any Gaussian form. Thus, it is quite natural that the description for the convergence to the SG phase fails if one tries to describe it in the same way as the dynamics which converges to the FMR phase. The convergence to the SG phase, if anything, can very effectively be described by assuming the phenomenological non-Gaussian form of the field distribution introduced in [26].

Acknowledgments

The author would like to thank Professor K Kaneko, Dr K Nemoto, Dr F H Willeboordse, Dr S Adachi and Professor H Sompolinsky for illuminating discussions, continual encouragements, critical reading of the manuscript and advice on the numerical computations. This work was financially supported by a Grant-in-Aid for Scientific Research on Priority Areas from the Ministry of Education, Science and Culture, Japan.

References

[1] Hopfield J 1982 *Proc. Natl Acad. Sci. USA* 79 2554
[2] Amit D J, Gutfreund H and Sompolinsky H 1985 *Phys. Rev. Lett.* 55 1930; 1987 *Ann. Phys., NY* 173 30
[3] Amit D J 1989 *Modeling Brain Function* (Cambridge: Cambridge University Press)
[4] Hertz J, Krogh A and Palmer R G 1991 *Introduction to the Theory of Neural Computation* (*Santa Fe Institute Studies in the Sciences of Complexity*) (Reading, MA: Addison-Wesley)
[5] Mézard M, Parisi G and Virasoro M 1987 *Spin Glass Theory and Beyond* (Singapore: World Scientific)
[6] Stein D L 1992 *Spin Glasses and Biology* (Singapore: World Scientific)
[7] Fukai T and Shiino M 1993 *Phys. Rev.* E **48** 867
[8] Crisanti A, Amit D J and Gutfreund H 1986 *Europhys. Lett.* 2 337
[9] Amari S and Maginu K 1988 *Neural Networks* 1 63
[10] Nishimori H and Ozeki T 1993 *J. Phys. A: Math. Gen.* 26 859
[11] de Dominicis C, Gabay M and Orland H 1981 *J. Physique Lett.* 42 L523
[12] de Dominicis C, Gabay M and Duplantier B 1982 *J. Phys. A: Math. Gen.* **15** L47
[13] Nishimura K and Nemoto K 1992 *J. Phys. A: Math. Gen.* 4 5561
[14] Sompolinsky H 1981 *Phys. Rev. Lett.* 47 935
[15] Parisi G 1980 *J. Phys. A: Math. Gen.* **13** L115
[16] Parisi G 1980 *J. Phys. A: Math. Gen.* **13** 1887
[17] Sherrington D and Kirkpatrick S 1975 *Phys. Rev. Lett.* 35 1792
[18] Sommers H-J and Dupont W 1984 *J. Phys. C: Solid State Phys.* 17 5785
[19] Tokita K 1993 *J. Phys. A: Math. Gen.* **26** 6915
[20] Ogielski A T and Stein D L 1985 *Phys. Rev. Lett.* 55 1634
[21] Tokita K 1993 Replica symmetry breaking and multivalley energy landscape in the Hopfield model *PhD Thesis* University of Tokyo
[22] Nemoto K 1987 *J. Phys. C: Solid State Phys.* **20** 1325
[23] Duplantier B 1981 *J. Phys. A: Math. Gen.* 14 283–5
[24] Bantilan F T and Palmer R G 1981 *J. Phys. F: Met. Phys.* 11 261
[25] Gardner E, Derrida B and Mattishaw P 1987 *J. Physique* **48** 741
[26] Henkel R D and Opper M 1991 *J. Phys. A: Math. Gen.* 24 2201